

# Reversible Solid Oxide Cell (ReSOC) as flexible polygeneration plant integrated with CO<sub>2</sub> capture and reuse

Giulio Buffo<sup>1,\*</sup>, Domenico Ferrero<sup>1</sup>, Massimo Santarelli<sup>1</sup>, and Andrea Lanzini<sup>1</sup>

<sup>1</sup>Dipartimento Energia, Politecnico di Torino – C.so Duca degli Abruzzi 24, 10129 Torino (Italy)

**Abstract.** This work presents the concept of a Reversible Solid Oxide Cell (ReSOC) system localized in an urban residential district. The system is operated as a polygeneration plant that acts as interface between the electricity grid and the local micro-grid of the district. The ReSOC plant produces hydrogen via electrolysis during periods of low electricity demand (i.e., low-priced electricity). Hydrogen is used for multiple city needs: public mobility (H<sub>2</sub> bus fleet), electricity production delivered to the micro-grid during peak-demand hours, and heat (accumulated in a storage) provided to the local district heating (DH) network. An additional option analyzed is the use of part of the H<sub>2</sub> to produce DME using CO<sub>2</sub> captured from biogas obtained from municipal solid wastes. The DME is used for fueling a fleet of trucks for the garbage collection in the residential district. A traditional CO<sub>2</sub> removal process based on liquid MEA thermally integrated with the ReSOC system is studied. A time-resolved model interfaces the steady-state operating points with the thermal storage and the loads (electrical, H<sub>2</sub> buses, DME trucks, heat), implementing constraints of thermal and H<sub>2</sub> self-sufficiency on the system. Neglecting the DME option, the average daily roundtrip electric efficiency is about 38%, while the annual efficiency, which includes H<sub>2</sub> mobility and thermal energy to DH, reaches 68%. When the DME option is considered, the thermal demand for CO<sub>2</sub> removal and conversion process reduces the heat availability for DH, while the need for additional H<sub>2</sub> for DME synthesis increases the electricity consumption for water electrolysis: both these phenomena imply a reduction of system efficiency (-9%) proportional to DME demand.

## 1 Introduction

Several strategies are studied to increase the flexibility of electricity grids and overcome the effects of supply-demand mismatch: some of these strategies follow the Power-to-X scheme, in which electricity is converted and stored not only for time-shifted power delivery, but also to cover non-electric demand in different sectors [1]. Among the X energy vectors to which electricity can be converted, hydrogen (H<sub>2</sub>) is a zero-emission energy carrier with several applications, either as it is (like in power sector and mobility) or as a platform molecule in chemical industry. For instance, the availability of H<sub>2</sub> can be integrated with the need for greenhouse gases emission reduction and the chemical recycling of CO<sub>2</sub> to sustainable fuels

---

\* Corresponding author: [giulio.buffo@polito.it](mailto:giulio.buffo@polito.it)

such as Di-Methyl Ether (DME), which can be used as a clean-burning potential Diesel pool additive [2] or even as an alternative fuel [3].

A H<sub>2</sub>-based polygeneration concept can follow different technological schemes: one is the Reversible Solid Oxide Cell (ReSOC) plant under examination, which fulfils both electrolysis and fuel cell requirements in a single component [4].

We developed a time-resolved model of the dynamic operation of a 10/50-MW (fuel cell/electrolysis) ReSOC polygeneration system integrated with CO<sub>2</sub> capture from biogas and conversion to DME in a residential district. The model interfaces the ReSOC operating points with a thermal storage unit and the diverse loads (power, H<sub>2</sub> buses, DME trucks and District Heating), adding the constraints of thermal and H<sub>2</sub> self-sufficiency of the system. On the basis of the plant simulation, a simple techno-economic assessment is presented.

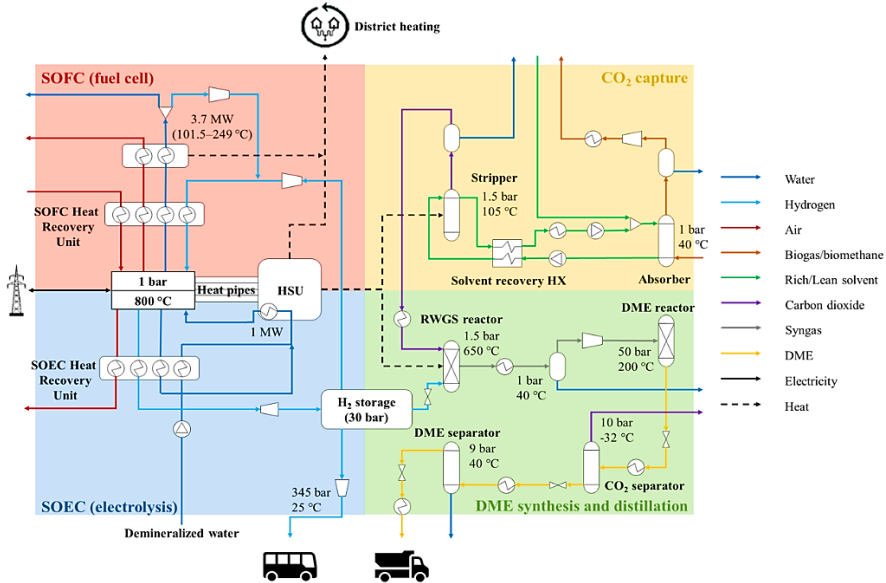


**Fig. 1.** Scheme of the ReSOC polygeneration system integrated with CO<sub>2</sub>-to-DME plant.

## 2 Methodology

The system has been simulated using the commercial process simulator Aspen Plus<sup>TM</sup>. A model for each of the four sections represented in Figure 1 was developed. Unlike the SOC system, the BoP operation is defined by the following constant specifications, notwithstanding that off-design performance would be more close to reality:

- Efficiency of isentropic compressors: 72%.
- Efficiency of hydraulic pumps: 54%.
- Efficiency of isentropic turbines: 71%.
- Pressure drop in heat exchangers: 0.05 bar.
- Efficiency of the inverter: 90%.

### 2.1 Steady-state model of the ReSOC system

The modeling approach followed for the thermo-electrochemical simulation of the SOC system is a lumped stack volume [5]. It simulates the shift of the operating point of the cells along the polarization curve, which is assumed with an exclusively ohmic behavior:

$$V_c(i) = V_{OC} - ASR i \quad (1)$$

The parameters that are constant in the model are the Area Specific Resistance,  $ASR = 0.241 \Omega \cdot \text{cm}^2$  [5] and the Open Circuit Voltage ( $V_{OC} = 0.952 \text{ V}$ ), with a symmetrical SOFC/SOEC polarization. In the SOFC model,  $\text{H}_2$  and  $\text{O}_2$  (21%<sub>v</sub> in ambient air) utilizations are equal to 80% and 90%, respectively; in SOEC model, water utilization is 60%.

The SOFC has been modeled as a stoichiometric reactor combined with a separator. The stoichiometric reactor simulates the oxidation of  $\text{H}_2$  into water with an air excess of 10% to avoid excessively low  $\text{O}_2$  partial pressure. In fact, instead of using cathodic air, the stack thermal management is performed by heat pipes: every heat pipe can transfer up to 740 W to the molten-NaCl Heat Storage Unit (HSU) under isothermal conditions [6]. To account for the separation of fuel and oxidant flows due to the interposed electrolyte in the real cells, nitrogen and unreacted  $\text{O}_2$  (cathode outlet in the real cell) are separated from the unreacted  $\text{H}_2$  and the water (anode outlet in the real cell) and vented. The exhaust anodic flow is recirculated to the stack with 3%<sub>v</sub> fraction of water to ensure humidification.

A similar approach was used for the reverse operating mode (electrolyzer). To avoid cathodic nickel oxidation, a reducing environment is ensured at the cathode inlet by partial recirculation of the  $\text{H}_2$ -rich cathodic exhaust. To avoid the risk of anode delamination due to excessively high concentrations of oxygen, preheated sweep air is injected into the anode with a flow rate assumed to be 15%<sub>v</sub> of the outlet oxygen produced by electrolysis.

Pinch analysis was performed for the integration of available heat sinks/sources.

## 2.2 Steady-state model of carbon capture section

This section consists of a two-column plant for the upgrade of a flow rate of biogas (65/35%<sub>v</sub>  $\text{CH}_4/\text{CO}_2$ ) with an amine-based solvent (30%<sub>w</sub> MEA, monoethanolamine). The two columns (an absorber to capture  $\text{CO}_2$  from the biogas stream and a stripper to cyclically regenerate the solvent) were modelled as rate-based reactors in Aspen Plus™, specifying the reactions involved, their kinetic and thermodynamic parameters [7]. The flow rate of lean solvent counterflowing biogas in the absorber is set to ensure a 98% removal of  $\text{CO}_2$  on a molar basis: the 97%<sub>v</sub> biomethane stream is assumed to be injected in the gas grid. The N3.0-pure stream of  $\text{CO}_2$  is flashed and conveyed to the Reverse Water-Gas Shift (RWGS) reactor.

## 2.3 Steady-state model of DME synthesis and distillation

The electrolytic  $\text{H}_2$  supplied by the storage ensures that the RWGS reaction ( $\text{CO}_2 + \text{H}_2 \rightarrow \text{CO} + \text{H}_2\text{O}$ ) yields a syngas with a  $\text{H}_2/\text{CO}$  ratio around 0.95. This condition maximizes the DME synthesis [8], occurring in a catalytic plug-flow reactor at 50 bar and 200 °C. The high fraction of DME in the product stream reduces the heat duty for the downstream cleaning process ( $\text{CO}_2$  separation, distillation of DME from residual  $\text{H}_2\text{O}/\text{MeOH}$  mixture) yielding a >99.99%<sub>v</sub> DME stream for automotive application.

## 2.4 Estimation of the energy demand of the residential district

A bottom-up stochastic model was developed taking the cue from the model by Richardson et al. [9] to generate 24 electric demand profiles of the district with time step of 1 minute, distinguishing weekdays (WD) and weekend days (WE) in the 12 months.

The demand of  $\text{H}_2$  for public transportation buses is presented in Table 1, assuming a consumption of 0.09  $\text{kg}_{\text{H}_2}/\text{km}$  [10]. The annual travelled distance is about 1 million km.

To fulfil the thermal demand estimated with the model by McKenna and Thomson [11], HSU supplies heat to a District Heating (DH) scheme with 120/90 °C supply/return temperature and thermal losses of 5%, operating from the 1<sup>st</sup> October to the 30<sup>th</sup> April.

Finally, it was estimated that a fleet of 44 trucks for the garbage collection in the studied residential district and in the surrounding area, with each truck traveling 50 km/day (i.e., 2,200 vehicles-km/day), consumes about 2,000 kg of DME every day.

**Table 1.** Daily demand of mobility H<sub>2</sub> (kg/day) in weekdays (WD) and weekend days (WE)

September-May (WD)	September-May (WE)	June-August (WD)	June-August (WE)
86.35	51.22	38.51	25.15

## 2.5 Time-resolved model of the polygeneration system

A time-resolved model interfaces the map of steady-state operating points with the temporal profiles of energy demand of the residential district.

### 2.5.1 Dynamic operation of the ReSOC plant

Priority was given to the production of mobility H<sub>2</sub> (SOEC mode) introducing a H<sub>2</sub> self-sufficiency constraint: the H<sub>2</sub> produced by the SOEC covers the H<sub>2</sub> consumed by the SOFC, the H<sub>2</sub> delivered to the buses and the H<sub>2</sub> for DME synthesis during each day.

The second level of priority was given to the electricity generation (SOFC mode) for the local micro-grid in the hours of peak demand on the electricity distribution grid.

The ReSOC plant is constrained to be also thermally self-sufficient: the heat stored in the HSU during SOFC operation (and in exothermic SOEC) is sufficient to sustain the eventual endothermic electrolysis of water and to pre-heat water feeding the SOEC stack.

The stack can operate in either fuel cell/electrolysis mode between 0% and 100% of the nominal load, with a constraint on the rate of change of the power output/supply ( $\pm 5\%$  of nominal power) during transients and excluding the option of a hot-standby.

The dynamic model simulates all the possible schedules of the plant per each of the 24 typical days – each WD and WE of the 12 months – with a time-step of 1 minute by assigning the operating mode and the power level of the stack (i.e., kW in SOEC or SOFC mode), considering a load-following regime in SOFC mode and an operation at a constant power rate in SOEC hours determined by the H<sub>2</sub> self-sufficiency constraint.

The ReSOC profiles that fulfill both the H<sub>2</sub> and thermal self-sufficiency constraints are valid. The profile with the highest number of hours of SOFC operation is considered per each typical day: in this case, the stack operates at high SOEC loads, close or over thermoneutrality (i.e., even with an additional heat supply to HSU).

### 2.5.2 Thermal management of the system

Since heat demand and supply do not always match, the plant includes a molten-NaCl buffer shifting heat stored at 800°C in time to minimize the amount of heat losses. Besides the in/out heat fluxes associated to the ReSOC operation, the HSU satisfies also the heat demand of the DH scheme, of the reboiler of CO<sub>2</sub> stripper and of the RWGS reaction.

The model estimates the number of houses requiring the residual heat in the HSU that exceeds the amount necessary to fulfil 100% of the thermal demand of the plant itself. In such way, the yearly energy balance on the HSU is satisfied.

## 3 Results

Setting the value of the nominal SOFC cell voltage to 0.77 V [12], a total of about 40,000 cells was necessary to obtain the nominal AC power of 10 MW<sub>e</sub>. Therefore, the resulting values for nominal cell voltage and current density in SOEC mode are 1.37 V and 1.74 A/cm<sup>2</sup>, respectively, corresponding to a SOEC/SOFC power ratio of 5.

To produce the DME necessary to feed 2,200 vehicles-km/day, 600 m<sup>3</sup>/h of biogas should be upgraded to capture about 126 m<sup>3</sup>/h of N3.0-pure CO<sub>2</sub>, which can undergo a RWGS reaction with 10 m<sup>3</sup>/h of H<sub>2</sub> to get a 0.95 H<sub>2</sub>/CO syngas ready for DME synthesis.

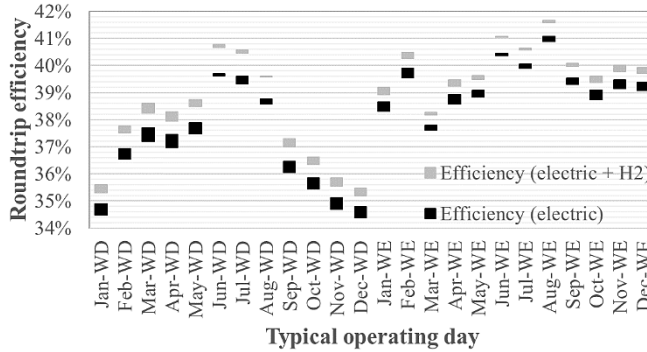


**Fig. 2.** Trend of the daily roundtrip (electric and global) efficiency throughout the year.

Two cases were analyzed: the first (case 1) neglecting CO<sub>2</sub> reuse pathway, the second (case 2) considering the entire plant as described in Figure 1.

In case 1, the daily roundtrip electric efficiency (i.e., the daily ratio of electricity generated during SOFC operation to electricity consumed during SOEC operation) is about 38%. Instead, the annual efficiency (which includes H<sub>2</sub> for the bus fleet and thermal energy to a DH scheme of 5,800 houses as useful commodities) reaches 68%. With respect to these benchmarks, the thermal demand of the CO<sub>2</sub>-to-DME process covered by the HSU implies a reduction of the heat availability for DH (the demand of only 4,300 houses can be met), while the need for additional H<sub>2</sub> for DME synthesis increases the electricity consumption for water electrolysis. All this implies a reduction of annual efficiency to 59% (case 2).

**Table 2.** Energy fluxes (in GWh/year) and global efficiency of the polygeneration system

	Case 1	Case 2
SOEC electric energy consumption	98.87	109.6
Electric energy consumption of the CO <sub>2</sub> -to-DME BoP	-	0.91
SOFC electric supply	37.83	37.34
DH thermal supply	26.28	19.48
Chemical energy of mobility H <sub>2</sub>	2.96	2.96
Chemical energy of mobility DME	-	5.83
Annual efficiency	67.84%	59.37%

A simple analysis of the economic feasibility was performed by assessing the balance between the expenditure for input electricity and the revenues from selling output electricity, H<sub>2</sub>, DH heat and DME. Market prices in Europe have been considered for the different energy vectors: 6 €/kg for H<sub>2</sub> (SMR H<sub>2</sub> as reference [13]), 600 €/ton for DME [14] and 69 €/MWh for DH heat [15]. For the electricity, the average market price of Italy in 2018 has been considered (61 €/MWh) [16], assuming that the purchasing price is 50% lower than the

average and the selling price is 20% higher. The results show that the plant is economically feasible, with a positive balance of 2.11 M€/year for case 1 and 1.68 M€ for case 2: the reduction of efficiency related to case 2 has a drawback on the economic performance. However, this balance does not take into account neither carbon credits nor the revenues from biomethane injection. Moreover, also grid balancing incomes and subsidies should be included in the analysis, making the plant more profitable in both cases. The detailed analysis was out of the scope of this work and will be carried out in future studies.

## 4 Conclusions

This work assessed the feasibility of a ReSOC polygeneration system for time-shifted power delivery and the production of mobility H<sub>2</sub>, integrated with a plant for the capture of CO<sub>2</sub> from biogas upgrading and its conversion to DME. A molten-NaCl storage integrated through a system of planar heat pipes manages the heat exchanged by the ReSOC: the excess thermal energy feeds a DH scheme.

The dynamic models generated a set of SOFC/SOEC schedules for every typical day. Of the schedules meeting the constraints of thermal and H<sub>2</sub> self-sufficiency, that with the highest number of hours of SOFC operation (i.e. maximizing heat availability) was studied. The integration of CO<sub>2</sub>-to-DME chain implied a -9% penalty with respect to the 68% annual efficiency of the system based only on the ReSOC plant. However, the adopted logic minimizes the thermal losses and allows relieving the grid by disconnecting local loads during peak hours, differentiating the input power in four energy carriers.

A simple techno-economic analysis confirmed the economic feasibility of the plant concept with an income of 1.68 M€/year with the integration of the CO<sub>2</sub>-to-DME chain.

## References

1. P. D. Lund, J. Lindgren, J. Mikkola, J. Salpakari, *Renew. Sustain. Energy Rev.*, **45**, 785–807 (2015)
2. G. Centi, S. Perathoner, in *Green Carbon Dioxide: Advances in CO<sub>2</sub> utilization*, 1–24 (Wiley, 2014)
3. G. A. Olah, A. Goepfert, G. K. S. Prakash, *Beyond Oil and Gas: The Methanol Economy* (Wiley-VCH, 2009)
4. S. Y. Gómez, D. Hotza, *Renew. Sustain. Energy Rev.*, **61**, 155–174 (2016)
5. A. Lanzini, D. Ferrero, M. Santarelli, in *Advances in Medium and High Temperature Solid Oxide Fuel Cell Technology*, 223–264 (Springer, 2017)
6. M. Dillig, J. Leimert, J. Karl, *Fuel Cells*, **14**, 479–488 (2014)
7. S. Moioli, L. A. Pellegrini, S. Gamba, *Procedia Engin.*, **42**, 1651–1661 (2012)
8. A. Farooqui, F. Di Tomaso, A. Bose, D. Ferrero, J. Llorca, M. Santarelli, *Energy Convers. Manag.*, **186**, 200–219 (2019)
9. I. Richardson, M. Thomson, D. Infield, C. Clifford, *Energy Build.*, **42**, 1878–1887 (2010)
10. Fuel Cell & Hydrogen Joint Undertaking, *Multiannual work plan 2014-2020* (2014)
11. E. McKenna, M. Thomson, *Appl. Energy*, **165**, 445–461 (2016)
12. P. Iora, M. A. A. Taher, P. Chiesa, N. P. Brandon, *Int. J. Hydr. En.*, **35**, 12680–12687 (2010)
13. C. Wulf, M. Kaltschmitt, *Sustainability* **10**, 1699 (2018)
14. V. Discacciati, S. Ferrari, Master Thesis (Politecnico di Milano, 2018)
15. O. Gudmundsson, J.E. Thorsen, L. Zhang, *WIT Trans Ecol Envir* 176, 3-13 (2013)
16. GME, [www.mercatoelettrico.org/it/Statistiche/ME/DatiSintesi.aspx](http://www.mercatoelettrico.org/it/Statistiche/ME/DatiSintesi.aspx), (24.06.2019)